Ionomeric Blends of Poly(ethyl acrylate-*co*-4-vinylpyridine) with Zinc-Neutralized Sulfonated Poly(ethylene terephthalate). 2. Effect of Specific Interactions upon the Crystalline Phase

C.-W. Alice Ng and William J. MacKnight*

Department of Polymer Science and Engineering, University of Massachusetts, Amherst, Massachusetts 01003

Received November 15, 1993®

ABSTRACT: The crystallization kinetics, melting behavior, and morphology of an ionomeric blend system of poly(ethyl acrylate-*co*-4-vinylpyridine) with zinc-neutralized sulfonated poly(ethylene terephthalate) were investigated. Partial compatibilization in this multiphase (semicrystalline) blend system was demonstrated in part 1[1] of this series of studies and was shown to be a result of the specific interactions among the ionic moieties incorporated along the chain backbone. Crystallization kinetics were studied using DSC, and an increase in the rate of crystallization was observed as a result of enhanced nucleation efficiency originating from the specific interacting sites as confirmed by the TEM study. The melting behavior observed from DSC analysis showed perturbation of crystal growth as reflected by the broadening of the melting endotherms, lowering of the melting temperatures, and reduction in the degree of bulk crystallinity due to the presence of the specific interactions. The structural organization of the crystalline phase was further examined with TEM. The spherulites for the modified blends were more abundant, less well developed, and smaller as compared to those of the unmodified, immiscible blends without the specific interactions.

Introduction

The results of the multiphase (semicrystalline) ionomeric blend study reported in part 1[1] of this investigation have unequivocally demonstrated the effectiveness of incorporating ionic moieties along polymer chain backbones to compatibilize immiscible polymer pairs, namely, poly(ethyl acrylate) (p(EA)) and poly(ethylene terephthalate) (PET). The nature and the degree of the specific interactions have been characterized and determined with Fourier transform infrared spectroscopy. The level of compatibility of the blends has been quantified using differential scanning calorimetry (DSC) and dynamic mechanical thermal analysis (DMTA). Results show that more favorable specific interactions lead to a higher degree of compatibility between the polymer pair. Despite the fact that the semicrystalline component can induce phase separation upon crystallization, thereby lessening the effect of the specific interactions in the polymer system, blend compatibilization is still observed.

In the present study, special emphasis is focused on the impact of the specific interactions upon the crystalline phase within the blend matrix. The crystallization of PET has been the subject of a great deal of interest in both the industrial and academic fields. The techniques for the enhancement of the crystallization rate of PET include the incorporation of heterogeneous nucleating agents such as polymer fibers,[2] inorganic oxides,[3] and organic salts.[4–6] The crystallization rate enhancement mechanism is said to involve the formation of "activated surfaces" to facilitate crystallization. Among the different types of "activated surfaces", ionic groups located at the ends of polymer chains were found to be capable of accelerating the crystallization rate of PET. On the basis of the above finding, it is postulated that the specific interactions (which are also ionic in nature) might induce similar rate enhancement upon the crystallization kinetics of a semicrystalline/amorphous ionomeric blend. Nevertheless, the crystallization of this ionomeric blend might be further complicated by the enhanced mixing of the polymer pair by virtue of the presence of the specific interactions. Therefore, efforts have been made to understand the complex relationship between the crystallization and the blend compatibilization of this semicrystalline/amorphous ionomeric blend. In this regard, the crystallization kinetics, melting phenomena, and the morphologies of the ionomeric blends are examined. It is anticipated that the results derived from this study will advance our understanding of the mechanism of specific interactions in compatibilizing polymer blends, in particular semicrystalline/amorphous ionomeric blends.

Experimental Section

Materials Used. The polymeric materials used in this investigation have been described in part 1 of this series; the same nomenclature of the blends is adopted. The characteristics of the component polymers and their blends are summarized in Tables 1 and 2, respectively. An ion-exchange procedure used to convert the sodium sulfonated PET into its zinc form was described in part 1. Blends were prepared in the same manner as described in part 1.

Crystallization Kinetics. A Perkin-Elmer DSC-7 was used for all DSC measurements and was calibrated with indium. All scans were run with samples ranging from 10 to 15 mg in weight under a nitrogen purge to prevent oxidative degradation. All samples were heated to 250 °C and held at this temperature for 10 min to ensure that the molten state had been reached. The samples were then rapidly cooled, at a rate of 500 °C/min, to the crystallization temperature, T_c. The heat evolved during the crystallization process was recorded as a function of time. The initial development of crystallization, denoted at time $t = 0$, was taken by assuming the final baseline as the baseline for the entire isotherm and projecting backward the final baseline to the forward edge of the crystallization isotherms. The crystallization isotherms were then analyzed by the Avrami equation.

Melting Behavior. The melting behavior of all the blends and zinc-neutralized sulfonated PET was examined using DSC. After crystallizing at various T_c's, the samples were quenched from T_c to 25 °C and then heated at a rate of 10 °C/min to 250 °C. The melting temperatures of the blends were taken as the peaks of the multiple melting endotherms.

Morphology. A very dilute (0.125–0.25% (w/v)) blend solution in hexafluoropropan-2-ol (HFIP) was prepared. A thin polymer film was made by casting the solution directly on a carbon-coated copper grid. The solvent was allowed to evaporate slowly in a saturated HFIP atmosphere for 3 h. The specimens

® Abstract published in *Advance ACS Abstracts*, April 1, 1994.

0024-9297/94/2227-3033$04.50/0

Table 1. Characteristics of Component Polymers

polymer	designation	mol % of VP	$\bar{M}_n$	$\bar{M}_w/\bar{M}_n$
poly(ethyl acrylate)	p(EA)	0	230 000	3.87
poly(ethyl acrylate-*co*-4-vinylpyridine) (5.2% VP)	p(EA-*co*-VP) (5.2% VP)	5.2	201 000	2.02
poly(ethyl acrylate-*co*-4-vinylpyridine) (10.6% VP)	p(EA-*co*-VP) (10.6% VP)	10.6	161 000	1.96
zinc-neutralized sulfonated PET (7% SO_3Zn)[a]	PET-SO_3Zn (7% SO_3Zn)			

[a] IV = 0.44 dL/g.

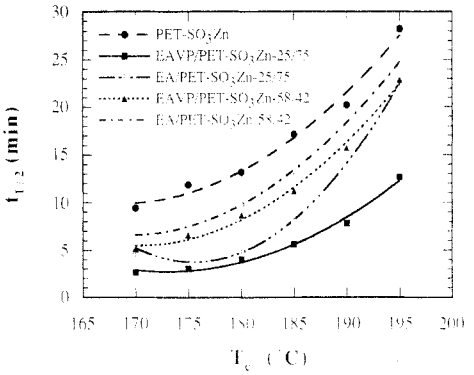

Figure 1. Crystallization kinetics: plots of $t_{1/2}$ versus T_c.

Table 2. Characteristics of Polymer Blends

polymer	mol % of VP	wt % of p(EA-*co*-VP)	wt % of (PET-SO_3Zn)
PET-SO_3Zn		0	100
EAVP/PET-SO_3Zn-25/75	10.6	25	75
EA/PET-SO_3Zn-25/75	0	25	75
EAVP/PET-SO_3Zn-58/42	5.2	58	42
EA/PET-SO_3Zn-58/42	0	58	42

were further annealed on a hot stage at 150 °C for 1 h under a nitrogen flow to optimize the crystallinity of the blend samples. The sample specimens were examined using a JEOL 100CX electron microscope operating at 100 keV.

Results and Discussion

Crystallization Kinetics. The isothermal crystallization kinetics of the polymers listed in Table 2 were investigated with DSC. This method was chosen because it required only small sample sizes and at the same time provided sufficient sensitivity to monitor the entire crystallization process.

The half-crystallization time, $t_{1/2}$, defined as the time required to attain half of the total crystallinity, was used as a measure of the rate of crystallization at a particular T_c, the crystallization temperature. The crystallization isotherms of the polymers were further analyzed by the Avrami equation:[7]

$$1 - X_t = \exp(-Zt^n) \tag{1}$$

$$\ln[-\ln(1 - X_t)] = n \ln t + \ln Z \tag{2}$$

$$Z = \ln 2/(t_{1/2})^n \tag{3}$$

where X_t is the crystallinity attained after time t, Z is the overall rate constant which is defined in eq 3, and n is the Avrami exponent, which is related to the mode of nucleation and the dimensionality of growth. In the calorimetric study, $X_t = A_t/A_\infty$, where A_t is the partial area recorded at time t and A_∞ is the total area under the isothermal curve. A graphical determination of n was made by plotting $\ln[-\ln(1 - X_t)]$ versus $\ln t$. The calculated values of the kinetics parameters are summarized in Table 3.

Figure 1 shows the plot of $t_{1/2}$ versus T_c for all the blends and zinc-neutralized sulfonated PET. For each polymer system, $t_{1/2}$ is found to increase with T_c. This indicates that the crystallization process is conducted in the nucleation-controlled regime. Nevertheless, the $t_{1/2}$ for all the blends is shorter than that for the zinc-neutralized sulfonated PET crystallizing at the same T_c. In particular, the $t_{1/2}$ for both modified blends is shorter than that for the corresponding unmodified blends crystallizing at the same T_c. In addition, the overall rate constant Z shown in Table 3 shows a similar trend as that of the $t_{1/2}$.

Table 3. Crystallization Kinetics Parameters

polymer	T_c (°C)	$t_{1/2}$ (min)	rate constant Z ($\times 10^4$) $(\text{min})^{1/n}$	Avrami exponent n
PET-SO_3Zn	195	28.2	0.6	2.9
	190	20.2	2.6	2.6
	185	17.2	12.0	2.3
	180	13.2	52.9	1.9
	175	11.9	22.5	2.3
	170	9.4	77.0	2.1
EAVP/PET-SO_3Zn-25/75	195	12.6	12.3	2.5
	190	7.8	68.0	2.2
	185	5.6	155.5	2.2
	180	4.0	416.2	2.0
	175	3.0	694.0	2.1
	170	2.6	989.6	2.0
EA/PET-SO_3Zn-25/75	195	23.1	0.5	3.1
	190	13.1	10.5	2.5
	185	7.9	88.8	2.2
	180	5.0	555.7	1.7
	175	4.7	655.5	1.7
	170	4.7	586.2	1.8
EAVP/PET-SO_3Zn-58/42	195	22.9	5.3	2.3
	190	15.7	34.6	1.9
	185	11.2	75.3	1.9
	180	8.7	169.2	1.7
	175	6.6	243.5	1.8
	170	5.1	391.4	1.8
EA/PET-SO_3Zn-58/42	195	25.3	5.9	2.3
	190	17.8	12.5	2.3
	185	12.7	91.1	1.9
	180	9.9	206.1	1.7
	175	8.9	137.2	1.9
	170	5.9	547.2	1.6

It is known that the sulfonate groups in PET-SO_3Zn aggregate to form multiplets or lower order clusters above a sulfonation level of 5 mol %.[8] Additionally, there has been experimental evidence about ionic groups located at the end of the polymer chains acting as nucleating sites, thereby accelerating the crystallization rate of polymers.[4-6] Sodium *o*-chlorobenzoate incorporated into PET is one example. Therefore, with the addition of the EA moiety into PET-SO_3Zn, some of the EA phase might be incorporated into the aggregates through ion–dipole interactions of the C=O from the acrylate group and the SO_3Zn group. On the basis of the above experimental findings, it is postulated that more effective nucleating sites are therefore formed in the unmodified blends, which could explain the enhanced crystallization rate as compared to that of the pure zinc-neutralized sulfonated PET. Nonetheless, the stronger zinc transition metal coordination complex involving the sulfonate groups and the vinylpyridine groups which is responsible for the enhanced mixing of the EAVP phase with the PET-SO_3Zn phase

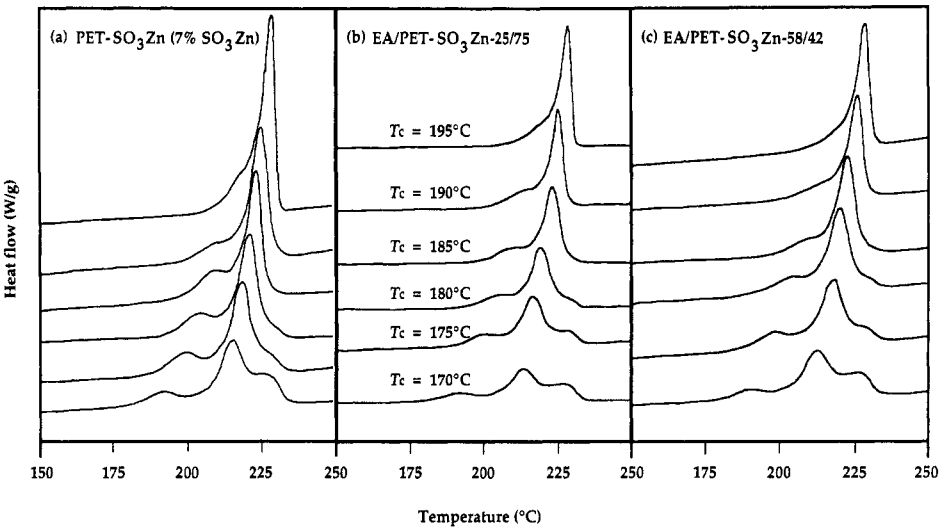

Figure 2. DSC melting curves for (a) PET-SO_3Zn (7 mol % SO_3Zn), (b) EA/PET-SO_3Zn-25/75, and (c) EA/PET-SO_3Zn-58/42 crystallized at the T_c indicated.

should provide even more stable and more effective nucleating sites for crystallization to take place. Therefore, this should further accelerate the crystallization rate of the PET component in the modified blends as compared to that of the unmodified counterparts. In agreement with this rationalization, it is observed that the crystallization rate of EAVP/PET-SO_3Zn-25/75 is indeed faster than that of the 58/42 blend crystallizing at the same T_c. This is obvious as the specific interactions among polymer chains are more favorable in the 25/75 blend as clearly shown by infrared spectroscopy in part 1.[1] Consequently, this results in higher nucleation efficiency, which further enhances the rate of crystallization.

As mentioned before, the crystallization kinetics were investigated in the nucleation-controlled regime. The observed trends of the crystallization rates among all the blends and PET-SO_3Zn should scale with the concentration of the nucleating sites in that the higher nucleation densities result in faster crystallization rates. This could be easily observed and demonstrated by examining the morphology of the blend system, which will be discussed in the later section.

With respect to the growth mechanism of the crystalline component in the blend, it is generally analyzed in terms of the Avrami exponent, n. According to the Avrami theory, the exponent n should be an integer which reflects a certain mechanistic behavior of crystal growth. However, nonintegral values of n were obtained in this study. Aside from experimental error, there are many other reasons for the discrepancy between the theoretical prediction and the actual crystallization phenomena of polymer systems.[9] However, it is believed that the Avrami exponent n, which may not adequately describe the actual mechanism of crystal growth, can still be useful for comparison purposes in this investigation.

As found in Table 3, the Avrami exponent n is approximately equal to 2 for all the blends and zinc-neutralized sulfonated PET for T_c = 170–185 °C. As T_c increases to higher temperatures, n is found to increase to nearly 3 except for EAVP/PET-SO_3Zn-58/42 and its unmodified counterpart, where n still remains about 2. This suggests that the crystal growth mechanism in zinc-neutralized sulfonated PET, EAVP/PET-SO_3Zn-25/75, and its unmodified counterparts is changing from one type to another within the range of T_c studied. However, for the EAVP/PET-SO_3Zn-58/42 and its unmodified counterparts, such change in growth behavior is not observed. On the basis of the above findings, it is postulated that the presence of the specific interactions among the polymer chains or specifically the modification of the nucleation mechanism does not exert a strong effect on the value of n in the range of T_c studied. Instead, the significant increase in the amount of a second phase, the EA or EAVP phase, might be responsible for the inhibition or retardation of the mechanistic change of crystal growth in the polymer matrix within the range of T_c investigated. However, a full explanation for this phenomenon is not available.

Melting Behavior. The melting behavior of the crystalline component in the blends and zinc-neutralized sulfonated PET was examined as a function of T_c using DSC. The samples were first isothermally crystallized at various T_c's ranging from 170 to 195 °C for sufficient time to ensure complete crystallization and were then quenched to room temperature. The samples were then heated at a rate of 10 °C/min beyond melting. With crystallization time up to 2 h, the subsequent DSC measurements can be assumed to reflect closely the crystal formation at the specified T_c.

Semicrystalline PET is known to exhibit classical multiple endothermic transitions, the lower endotherm being approximately 10–20 °C above the annealing temperature.[10] The lower endotherm has been associated with a discontinuous crystallite size distribution, which is very sensitive to the annealing conditions. Roberts[10] presented evidence for a reorganization mechanism. As the annealing temperature approached the higher endothermic transition, only a single endothermic transition was observed, which appeared at higher T_m. As shown in Figure 2a, the zinc-neutralized sulfonated PET used in this study also exhibits multiple melting endotherms and similar behavior upon annealing. In Figures 2 and 3, it is shown that for all the blends and zinc-neutralized sulfonated PET, there is an increased contribution to the higher endothermic transitions when crystallized at progressively higher T_c, and the values of T_m increase accordingly. This is due to higher molecular mobility of the system at higher T_c, which has already been observed in pure PET.[10] However, for both unmodified blends and pure zinc-neutralized sulfonated PET, as shown in Figures 2a–c, similar melting behavior with respect to the shape and peak width of the endotherms is observed for samples crystallized at the same T_c except that the melting peaks occur at slightly lower temperatures for the unmodified

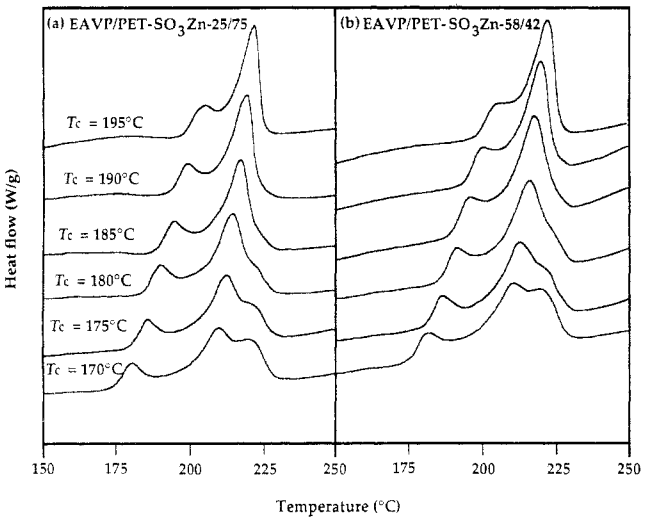

Figure 3. DSC melting curves for (a) EAVP/PET-SO_3Zn-25/75 and (b) EAVP/PET-SO_3Zn-58/42 crystallized at the T_c indicated.

Table 4. Enthalpy of Melting of All Polymer Blends and Sulfonated PET Crystallized at Specified T_c

	normalized ΔH_m[a] (J/g)					
polymer	170 °C	175 °C	180 °C	185 °C	190 °C	195 °C
PET-SO_3Zn	32.2	35.9	35.8	35.6	35.4	41.7
EAVP/PET-SO_3Zn-25/75	28.0	27.2	27.8	26.0	25.3	23.5
EA/PET-SO_3Zn-25/75	34.5	35.2	37.5	38.9	37.2	41.1
EAVP/PET-SO_3Zn-58/42	29.8	28.0	28.0	27.1	25.3	24.3
EA/PET-SO_3Zn-58/42	33.4	34.4	35.8	34.9	29.6	30.4

[a] ΔH_m is normalized per gram of PET-SO_3Zn.

blends. This suggests that the crystallite sizes and distribution within the unmodified blend matrix are very similar to those of zinc-neutralized sulfonated PET. But in view of the slight depression of melting peak temperatures in the unmodified blends, their crystals are considered to be slightly less perfect than those of pure sulfonated PET, possibly due to the presence of the EA phase. However, it is believed that the crystals are growing in localized regions within the polymer matrix, preferentially in the sulfonated PET rich phase in order to achieve a similar crystal growth environment and perfection as in pure sulfonated PET. In this respect, the similarity in melting phenomenon serves as an indicator of incompatibility in the unmodified blends.

Unlike the unmodified blends and zinc-neutralized sulfonated PET, both modified blends show very different melting patterns as shown in Figure 3. The melting endotherms appear broader, and the peak temperatures are several degrees lower. Especially at higher T_c, the crystals in the unmodified blends can attain higher perfection as shown by the sharpness of the melting transitions. Thus, it is apparent that the presence of specific interactions between polymer chains significantly interrupts the crystal growth process, which is manifested by the much broader endotherms and a relatively larger contribution to the lower temperature endotherm for samples crystallizing at the same T_c. This perturbation of crystal growth arising from specific interactions provides additional evidence for the compatibility of these modified blends.

It is found that the normalized melting enthalpy based on the multiple endotherms is in general lower for the modified blends than that of the unmodified counterparts. The results for the blends and zinc-neutralized sulfonated PET are shown in Table 4 and Figure 4. Again this behavior can be associated with the presence of specific interactions between polymer chains which decreases the

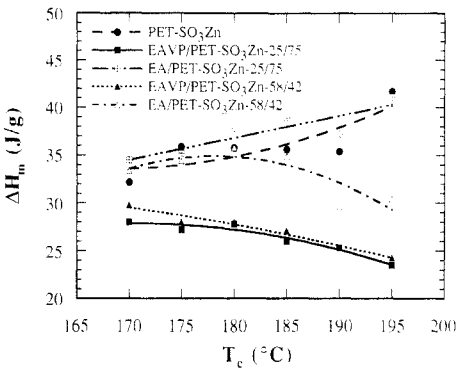

Figure 4. Normalized ΔH_m versus T_c.

crystallizability of the PET component in the modified blends. In addition, it is interesting to find that the ΔH_m values for the modified blends show a monotonic decrease with increasing T_c, unlike that observed in the case of PET-SO_3Zn. These phenomena further show that the presence of specific interactions reduces the crystallizability of the blend system, even though the polymer chains have higher mobility at higher T_c. On the basis of the results of the bulk crystallinity and kinetics studies, it is interesting to note that the specific interactions enhance the crystallization rate of the semicrystalline component and at the same time reduce the crystallinity of that component in the blend. One possible explanation could be that the nucleation densities induced by the presence of specific interactions are so high that the crystallites grow very fast simultaneously but in a chaotic manner, leaving little space for further crystal growth and thus giving rise to an overall lowering of the bulk crystallinity.

Morphology. The morphologies of the polymer blends, both modified and unmodified, were examined using transmission electron microscopy (TEM). It is anticipated that with this technique the impact of the specific intermolecular interactions between the polymer pair can be discriminated through the differences in the morphologies of the blends.

As presented in Figures 5–8, spherulite formation is clearly observed in all the blends with sufficient electron density contrast between the amorphous region consisting of both the EA or EAVP and zinc-neutralized sulfonated PET components and the crystalline region. This is indeed a unique feature about this blend system in that it does not require sample pretreatments such as staining and chemical etching for proper imaging. Unlike the blends, the zinc-neutralized sulfonated PET would require staining to provide the necessary contrast to image the spherulites.

It must be recognized that the morphologies revealed by TEM show only the phase relationship between the crystalline region of zinc-neutralized sulfonated PET and the amorphous region of both the EA or EAVP phase and zinc-neutralized sulfonated PET, but not the individual phases of zinc-neutralized sulfonated PET and EA or EAVP. Nevertheless, it is hoped that the organization of the spherulites can give some information about the phase behavior of the polymer pair.

In the blends of EA/PET-SO_3Zn-25/75 and EAVP/PET-SO_3Zn-25/75, the lower magnification TEM pictures in Figures 5a and 6a respectively show two different phase morphologies. In the unmodified blend, spherical domains of about 3 μm in diameter are observed. Spherulites are mostly localized in those spherical regions, with a few residing along the boundaries of each domain. However, spherical domains are not observed for the modified blend. Instead, the spherulites are found to be dispersed through-

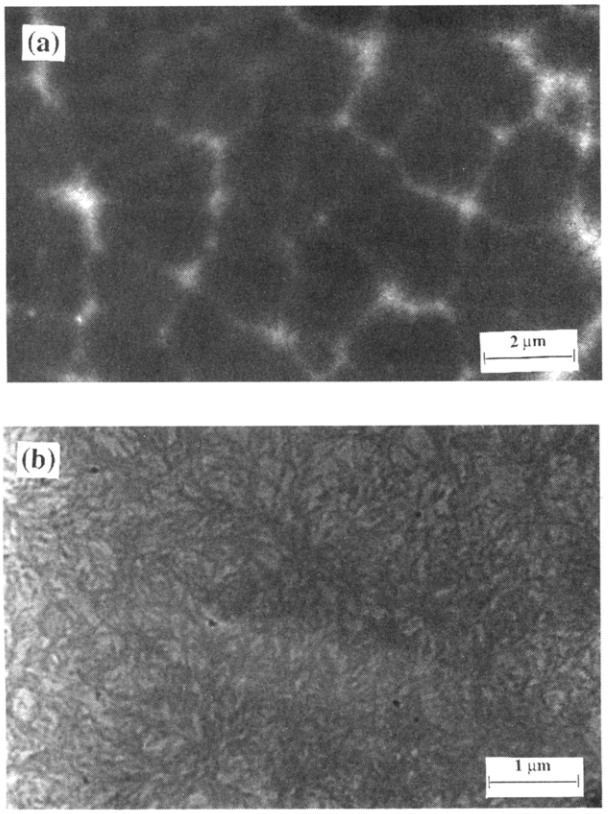

Figure 5. TEM pictures for EA/PET-SO_3Zn-25/75: (a) low and (b) high magnifications.

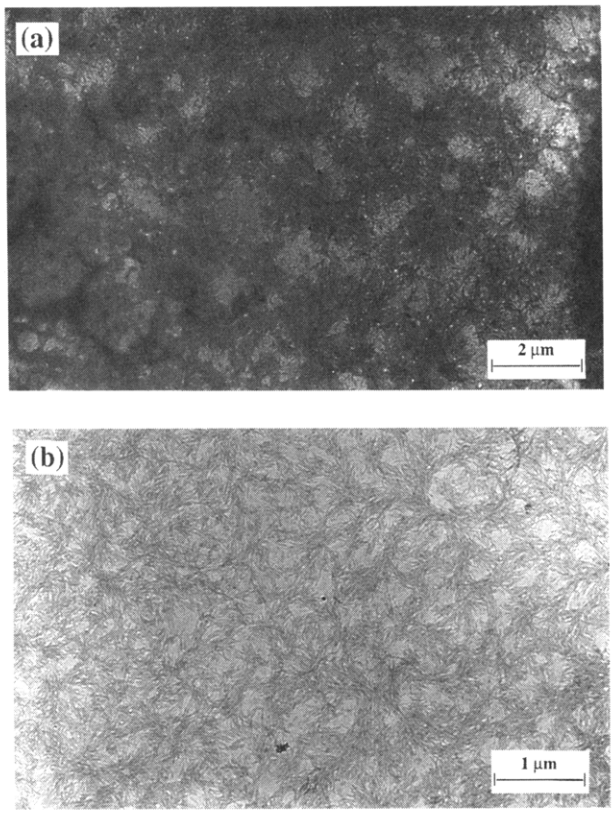

Figure 6. TEM pictures for EAVP/PET-SO_3Zn-25/75: (a) low and (b) high magnifications.

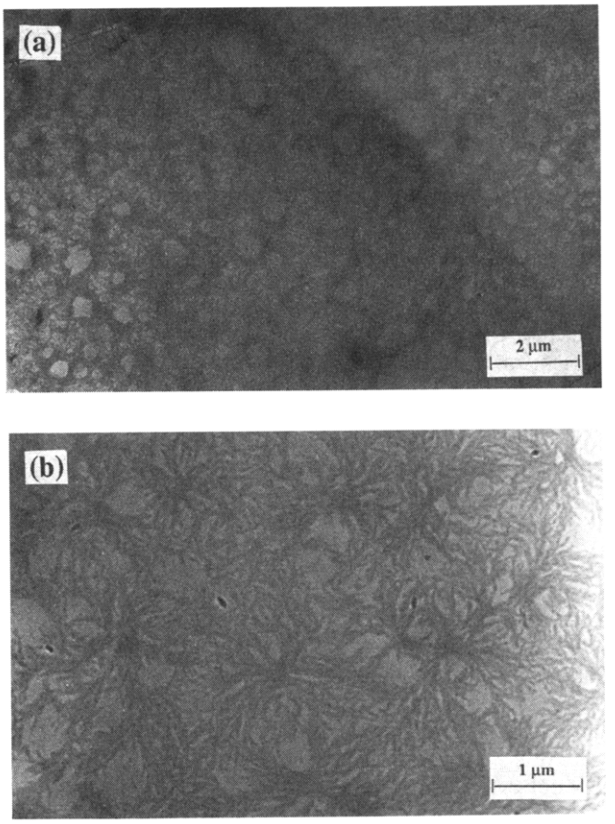

Figure 7. TEM pictures for EA/PET-SO_3Zn-58/42: (a) low and (b) high magnifications.

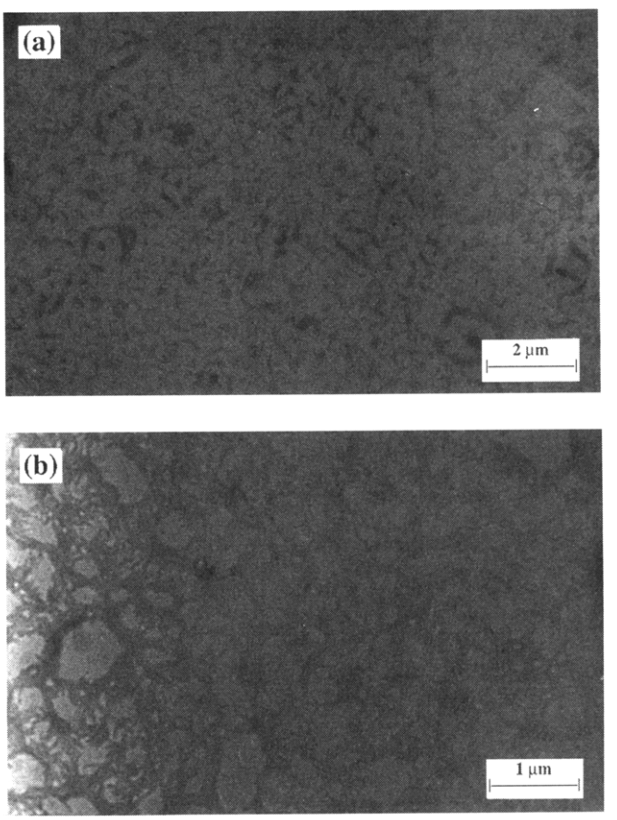

Figure 8. TEM pictures for EAVP/PET-SO_3Zn-58/42: (a) low and (b) high magnifications.

out the polymer matrix. In Figure 7a, similar spherical domains are observed for EA/PET-SO_3Zn-58/42 but they are not as pronounced as in the 25/75 blend. In Figure 8a, the low magnification view also shows a more disperse distribution of spherulites in EAVP/PET-SO_3Zn-58/42 as compared to its unmodified counterparts. But again this is not as pronounced as in the 25/75 counterparts.

With the morphologies examined under higher magnification, as shown in Figures 5b, 6b, 7b, and 8b, more subtle features are revealed. It is found that the spherulites of the unmodified blends are in general larger and better

developed, and their branches are thicker than those of their counterparts. This strongly supports the fact that the absence of strong specific interactions between the polymer pairs leads to a less interrupted crystal growth process as manifested by the melting behavior presented previously. On the other hand, as the EA phase or EAVP phase increases, the spherulites become more open, which indicates that more of the second phase is incorporated within the spherulites of the crystalline component. Another important feature observed is that the density of spherulites is found to be lower in the unmodified blends. This confirms the hypothesis stated earlier that the nucleation density for crystal growth is lower in the unmodified blends. This further demonstrates the notion previously discussed that specific interactions act as nucleating sites to enhance the rate of crystallization of the PET component within the polymer matrix.

Conclusion

An ionomeric blend system of poly(ethyl acrylate-*co*-4-vinylpyridine) with zinc-neutralized sulfonated PET was investigated with special emphasis on the impact of the specific interactions upon the crystalline phase of the polymer system. From the kinetics studies, the semicrystalline component (zinc-neutralized sulfonated PET) is found to crystallize at a faster rate under a nucleation-controlled mechanism due to enhanced nucleation efficiency originating from the specific interacting sites. On the other hand, increased amounts of the EA or EAVP phase are shown to be able to influence the crystallization mechanism of the PET component in the polymer matrix at high T_c. Further, the melting behavior of the blends is significantly modified as the interchain interactions interfere with the crystallization process of the PET component in the matrix. This in turn leads to a decrease in the degree of crystallinity and T_m and a broadening of the melting endotherms. In summary, the presence of specific interactions enhances the rate of crystallization without affecting the crystallization mechanism but does reduce the crystallizability of the system. The morphology, examined by TEM, of the blends is altered as a result of the ionic modification. The spherulites are observed to be less well developed, smaller in size, and denser in population due to the compatibility of the two polymer phases.

Acknowledgment. The authors gratefully acknowledge the financial support received from the Materials Research Laboratory at the University of Massachusetts, supported by the National Science Foundation.

References and Notes

(1) Ng, C.-W. A.; Lindway, M. J.; MacKnight, W. J. *Macromolecules*, preceding paper in this issue.
(2) Przygocki, W.; Wlochowicz, A. *J. Appl. Polym. Sci.* **1975**, *19*, 2683.
(3) Reinsch, V. E.; Rebenfeld, L. *Polym. Mater. Sci. Eng.* **1993**, *68*, 182.
(4) Legras, R.; Bailly, C.; Daumerie, M.; Dekoninck, J. M.; Mercier, J. P.; Zichy, V.; Nield, E. *Polymer* **1984**, *25*, 835.
(5) Legras, R.; Dekoninck, J. M.; Vanzieleghem, A.; Mercier, J. P.; Nield, E. *Polymer* **1986**, *27*, 109.
(6) Dekoninck, J. M.; Legras, R.; Mercier, J. P. *Polymer* **1989**, *30*, 910.
(7) Avrami, M. *J. Chem. Phys.* **1939**, *7*, 1103; **1940**, *8*, 212; **1941**, *9*, 177.
(8) Ostrowska-Czubenko, J.; Ostrowskz-Gumkowska, B. *Eur. Polym. J.* **1988**, *24* (1), 65.
(9) Grenier, D.; Prud'homme, R. E. *J. Polym. Sci., Polym. Phys. Ed.* **1980**, *18*, 1655.
(10) Roberts, R. C. *Polymer* **1969**, *10*, 113.